

# Interacting Dirac Fermions on Honeycomb Lattice

Wei Wu<sup>1</sup>, Yao-Hua Chen<sup>1</sup>, Hong-Shuai Tao<sup>1</sup>, Ning-Hua Tong<sup>2</sup>, and Wu-Ming Liu<sup>1</sup>

<sup>1</sup>*Beijing National Laboratory for Condensed Matter Physics,*

*Institute of Physics, Chinese Academy of Sciences, Beijing 100190, China*

<sup>2</sup>*Department of Physics, Renmin University of China, Beijing 100872, China*

(Dated: February 23, 2024)

We investigate the interacting Dirac fermions on honeycomb lattice by cluster dynamical mean-field theory (CDMFT) combined with continuous time quantum Monte Carlo simulation (CTQMC). A novel scenario for the semimetal-Mott insulator transition of the interacting Dirac fermions is found beyond the previous DMFT studies. We demonstrate that the non-local spatial correlations play a vital role in the Mott transition on the honeycomb lattice. We also elaborate the experimental protocol to observe this phase transition by the ultracold atoms on optical honeycomb lattice.

PACS numbers: 71.27.+a, 71.30.+h, 71.10.Fd

The honeycomb lattice systems have been intensively studied recently, where a number of exotic phenomena are found in both experiment and theory, such as the single-layer graphene [1–3], the topological Mott insulator [4] and the recently found quantum spin liquid [5]. The electrons on honeycomb lattice can be described by a “relativistic” massless Dirac-fermion model [6], which is characterized by the linear low-energy dispersion relation  $E(\mathbf{k}) = \pm v_F |\mathbf{k}|$ . For half-filling case, the Fermi surface of honeycomb lattice is reduced to isolated points at the corners of Brillouin zone, hence the density of states vanishes at the Fermi level, leading to the so called semimetal. When the repulsive interaction between the fermions is turned on, one can expect this semimetal to be driven into a gapped insulator by the sufficient strong interaction, in other words, a semimetal-Mott insulator transition happens. The Dirac fermion on honeycomb lattice is massless, hence the prevalent Fermi liquid theory is not proper here. Moreover, the semimetal has a small spectral weight near the Fermi surface, thus the low-energy many-body scattering effects would be quite different from those of the usual metallic systems. As a consequence of these anomalous natures, a new scenario is desirable for the description of Mott transition of the interacting Dirac fermions. There have been various theoretical studies of phase transitions on the honeycomb lattice, however up to date no comprehensive conclusion has been achieved [7–9].

Due to the efficient description of the quantum fluctuations, the DMFT [10–13] and its cluster extensions [14–16] have made substantial progress in the field of Mott transition in the past decades. The recent DMFT studies on honeycomb lattice find a first-order Mott transition and the renormalization of the Fermi velocity  $v_F$  induced by the interaction [17, 18]. Nevertheless, the DMFT ignores the non-local correlations. It is efficient only in physical systems with high dimensions or large coordination numbers [10]. The CDMFT method [14], as a cluster extension of DMFT, effectually incorporates the spatial correlations by mapping the lattice problem into

a self-consistently embedded cluster rather than a single site in DMFT. For low-dimensional systems, the quantum fluctuations are much stronger than in the higher dimensions, hence the CDMFT method is more precise than the DMFT here. To our knowledge, the DMFT calculations on square lattice basically agree with the CDMFT. The local approximation of DMFT captures well the main characteristics of the first-order Mott transition [19]. However, in the 1D chain lattice, the ignorance of non-local correlations within DMFT leads to results with severe errors [20]. The coordination number of honeycomb lattice is three which is between those of 2D square lattice and 1D chain lattice. Therefore, it is interesting to see whether the non-local correlations can significantly affect the behaviors of the electrons on honeycomb lattice and whether the CDMFT can provide novel results beyond the DMFT.

In this Letter, we combine the CDMFT method with CTQMC simulation [21], which is employed as impurity solver, to investigate the interacting Dirac fermions. A second order Mott transition is suggested. We also find a number of novel features of the Dirac fermions, including the quasi-particles with anomalous long lifetime and the invariable density of low-energy excitations which is highly relevant to the non-local correlations. Our results are distinct from those of the previous DMFT studies [17, 18], which indicate the non-local correlations are indeed crucial in the honeycomb lattice.

We consider the standard Hubbard model on the honeycomb lattice defined by the Hamiltonian,

$$H = -t \sum_{\langle i,j \rangle, \sigma} c_{i\sigma}^\dagger c_{j\sigma} + U \sum_i n_{i\uparrow} n_{i\downarrow} + \mu \sum_i c_{i\sigma}^\dagger c_{i\sigma}, \quad (1)$$

where  $c_{i\sigma}^\dagger$  and  $c_{i\sigma}$  are the creation and the annihilation operator of fermions with site index  $i$  and spin index  $\sigma$ ,  $n_{i\sigma} = c_{i\sigma}^\dagger c_{i\sigma}$  is the density operator.  $U$  is the on-site repulsion, and  $\mu$  is the chemical potential. The nearest neighbor hopping amplitude  $t$  ( $t > 0$ ) determines the bare dispersion of the honeycomb lattice

$$E(\mathbf{k}) = \pm t \sqrt{3 + 2\cos(k_y a) + 4\cos(\sqrt{3}k_x a/2)\cos(k_y a/2)},$$

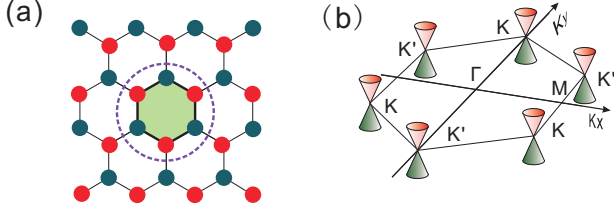


FIG. 1: (Color online). a) Illustration of the honeycomb lattice. The dashed line sketches the 6-site cluster scheme we explore in this work. b) The first Brillouin zone of the honeycomb lattice. The linear low-energy dispersion relation displays conical shapes near the Fermi level.

where  $a$  is the distance between the two adjacent sites, the plus and minus sign respectively denotes the upper ( $\pi$ ) and lower ( $\pi^*$ ) band. At low energies, the dispersion relation can be approximated as a linear one  $E(\mathbf{k}) = \pm v_F |\mathbf{k}|$ , which can be described by the Dirac cones as shown in Fig. 1b. We take  $t$  as the energy unit throughout this paper.

The CDMFT method has been successfully applied to the studies on Mott transition of the Hubbard model for various systems [22–24]. We use CDMFT to map the original honeycomb lattice onto a 6-site effective cluster embedded in a self-consistent medium. The effective cluster model is obtained via an iterative procedure which can be started with a initial guess of the cluster self-energy  $\Sigma(i\omega)$ . The effective medium represented by the Weiss function  $g(i\omega)$  is determined by the cluster self-energy  $\Sigma(i\omega)$  via the coarse-grained Dyson equation,

$$g^{-1}(i\omega) = \left( \sum_{\mathbf{K}} \frac{1}{i\omega + \mu - t(\mathbf{K}) - \Sigma(i\omega)} \right)^{-1} + \Sigma(i\omega), \quad (2)$$

where  $t(\mathbf{K})$  is the Fourier-transformed  $6 \times 6$  hopping matrix with wavevector  $\mathbf{K}$  in the cluster reduced Brillouin zone of the superlattice, and  $\mu$  is the chemical potential. Since the effective cluster model has been defined by  $g(i\omega)$ , we can employ the numerical methods [21, 25–27] as impurity solver to calculate the cluster Green's function  $G(i\omega)$ . By using Dyson equation  $\Sigma(i\omega) = g^{-1}(i\omega) - G^{-1}(i\omega)$ , we then recalculate the cluster self-energy  $\Sigma(i\omega)$  to close the self-consistent iterative loop. This CDMFT loop is repeatedly iterated until the numerical convergence has been achieved. In the present work, we use the numerically exact CTQMC simulation as impurity solver and take about  $7 \times 10^7$  QMC sweeps for each CDMFT loop.

We first study the density of states (DOS) derived from the imaginary time Green's function  $G(\tau)$  by using maximum entropy method [28]. The DOS for several values of on-site interaction  $U$  at temperature  $T/t = 0.05$  are presented in Fig. 2. When the interaction is increased, the two quasi-particle peaks above and below Fermi level

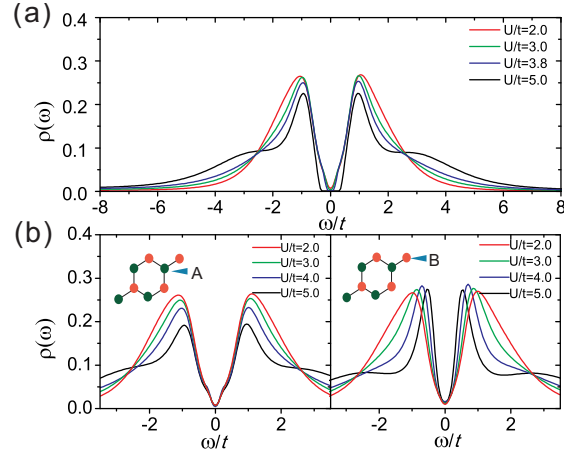


FIG. 2: (Color online). The density of states for different interaction strength  $U$  at temperature  $T/t = 0.05$ . a) Within 6-site CDMFT, the DOS near Fermi level is invariable until the Mott transition happens, which denotes a constant Fermi velocity  $v_F$  in the semimetal regime. b) The 8-site cluster results. Insert: geometry of the 8-site cluster. Left panel: the low-energy DOS of central site A is invariable with the increasing of  $U$ , which agrees with the 6-site CDMFT result. Right panel: the low-energy DOS of boundary site B increases as  $U$  increases, resembling the DMFT result. Note that the Mott transition critical value  $U_c$  of the 8-site cluster is much larger than that of the 6-site cluster and close to the DMFT result. This is due to the boundary effects.

shift to the Fermi surface. The spectral weight is continuously transferred to the higher energy states, and eventually a gap opens at the Mott transition critical value  $U_c/t \sim 3.7$ . However, it is surprisingly noted that the DOS near Fermi level is independent of the interaction strength  $U$  until the Mott transition happens. The quasi-particles in semimetal regime are always analogous to the non-interacting Dirac gas, indicating no renormalization of the Fermi velocity. This result is completely different from the previous DMFT studies [17, 18], where the results suggest the DOS near Fermi level increases as  $U$  increases in the semimetal region, hence the Fermi velocity  $v_F$  is renormalized by the on-site interaction. We argue that the non-local correlations which are absent in DMFT, but included effectively by CDMFT significantly reduce the low-energy spectral weight.

To clarify the spectral reduction effect of the non-local correlations, we study an 8-site cluster which has two boundary sites with only one neighbor site in the cluster. The geometry of the 8-site cluster is shown in inserts of Fig. 2b. It is apparent that the reduction of the coordination number subdues the non-local correlations for boundary sites [29], therefore the characters of the boundary sites may be distinguished from those of the central sites. As shown in Fig. 2b, the central site shows invariable low-energy DOS coinciding with the 6-

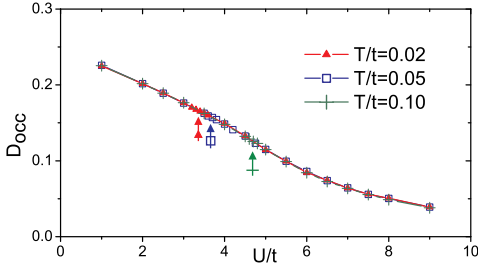


FIG. 3: (Color online). Double occupancy  $D_{occ}$  as a function of interaction  $U$  at different temperatures. The double occupancy is insensitive to temperature for both weak- and strong-coupling regime, hence the three curves for temperature  $T/t = 0.02, 0.05, 0.10$  strictly superpose each other. The double occupancies decrease smoothly as  $U$  increases, indicating second-order Mott transitions. The transition points for different temperatures are marked by the arrows.

site CDMFT study. However, the result of boundary site suggests low-energy DOS increasing as  $U$  increases, which is just a characteristic observed by the DMFT. The central and boundary sites are studied in one cluster, this disparity can only be attributed to the non-local correlations. We therefore conclude that the DMFT incorrectly suggests an increasing low-energy DOS due to the ignorance of the non-local correlations.

We further investigate the double occupancy defined by the first derivative of the free energy  $F$ ,  $D_{occ} = \frac{\partial F}{\partial U} = \langle n_{i\uparrow} n_{i\downarrow} \rangle$  as a function of  $U$  for different temperatures. As shown in Fig. 3, we find that when the temperature is lower than  $T_c/t \sim 0.1$ , the  $D_{occ}$  is independent of  $T$  in both semimetallic and insulating phase. Unlike the DMFT result [18] or CDMFT studies on triangular lattice [22] and kagomé lattice [24], where the double occupancies  $D_{occ}$  are insensitive to the temperature in only insulating phase. It is also remarkable that when  $U$  increases, the  $D_{occ}$  curves decrease smoothly on the entire domain of  $U$  which indicates second-order phase transitions. There is no hysteresis phenomenon observed in our calculations, which also signals continuous phase transitions. This feature is expected, considering the fact that regardless of the on-site interaction strength, the upper and lower Hubbard band of honeycomb lattice always touch each other in only Dirac points in the semimetallic phase. Therefore the order parameter  $D_{occ}$  decreases continuously even when the gap between the two Hubbard bands opens.

Fig. 4 shows the spectral functions  $A(k, \omega)$  at  $K$  point  $k = (0, 4\pi/3a)$ ,  $M$  point  $k = (2\sqrt{3}\pi/3a, 0)$  and  $\Gamma$  point  $k = (0, 0)$ . For the  $K$  point (Dirac point), as the interaction  $U$  is increased,  $U/t = 3.0$  for example, the quasi-particle peak at Fermi surface ( $\omega = 0$ ) is strongly suppressed by the antiferromagnetic correlations, and a pseudogap develops. When  $U$  reaches the critical value

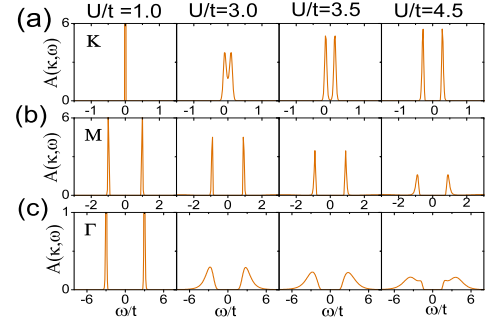


FIG. 4: (Color online) The spectral functions  $A(k, \omega)$  for a)  $K$  point. We can see the pseudogap at Fermi level developing as the interaction strength  $U$  increases. b)  $M$  point. The peaks of  $A(k, \omega)$  are very sharp even in the strong coupling regime, which indicates well-defined quasi-particles. c)  $\Gamma$  point. Far away from the Fermi level, the quasi-particle peaks are rapidly broadened by the interaction.

$U_c/t \sim 3.7$  for the phase transition, the pseudogap eventually engulfs the whole Fermi surface and the system turns into Mott insulator. The observation of pseudogap on the Dirac point in the transition regime indicates the antiferromagnetic correlations are the origin of the Mott phase transition. Note that while the quasi-particle peaks at  $\Gamma$  point are rapidly broadened by the on-site interaction, the spectral functions  $A(k, \omega)$  at the  $K$  and  $M$  point have sharp peaks even in the strongly coupling regime, indicating a long quasi-particle lifetime. This is related to the fact that there are few electrons near the Dirac points, thus the many-particle scattering effects are not prominent for the  $K$  and  $M$  points.

Although the local density of states  $\rho(\omega) = \sum_k A(k, \omega)$  is independent of the interaction for small energy  $\omega$ , the states are redistributing in the momentum space when the interaction increases. As shown in Fig. 5a, the distribution of quasi-particles with energy  $\omega/t = 0.4$  near a Dirac point  $(2\sqrt{3}\pi/3, 2\pi/3)$  becomes isotropic in different directions when  $U$  increases and finally the spectra averagely distribute in the whole ring. The Fermi surface denoted by  $A(k, \omega/t = 0)$  is also presented. The first Brillouin zone of honeycomb lattice has three  $K$  and three  $K'$  points located at the corners of the hexagon, as shown in Fig. 1b. Due to the particle-hole symmetry, the six Dirac points are actually all equivalent in our study. As a result, the Mott phase transition happens isochronously on the six Dirac points. Fig. 5b also shows that the locations of Dirac points are steady in momentum space with the increasing of interaction  $U$ .

Finally, we present the phase diagram of the interacting Dirac fermions on honeycomb lattice. The diagram is separated into semimetallic and insulating phases by the second-order Mott transition line. The critical value  $U_c$  decreases as temperature  $T$  decreases, and a finite  $U_c/t \sim 3.3$  for zero temperature phase transition is sug-

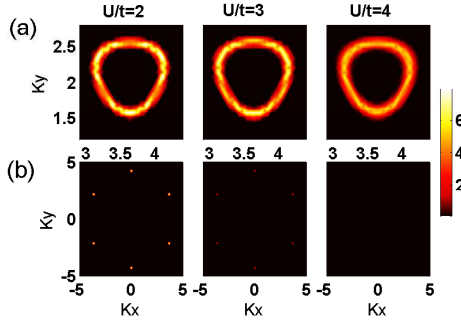


FIG. 5: (Color online) The distribution of  $A(k, \omega)$  in momentum space for different interactions. a) The distribution of  $A(k, \omega/t = 0.4)$  near a Dirac point  $(2\sqrt{3}\pi/3, 2\pi/3)$  becomes isotropic in different directions when  $U$  increases. b)  $A(k, \omega/t = 0)$  depicts the Fermi surface of honeycomb lattice reduced to six Fermi points.

gested, which is quite agree with the large scale quantum Monte carlo result  $U_c/t \sim 3.5$  [5]. Comparing to the DMFT result  $U_c/t \sim 10$  [18], the Mott transition critical value  $U_c$  within CDMFT is much smaller, and more reasonable according to the previous studies [7–9].

On the experiment side, due to the high controllability and clearness, the interacting ultracold atoms on the optical honeycomb lattice may be an ideal tool for the verification of our results [30–32]. The optical honeycomb lattice can be produced by three intersected standing-wave lasers. Each of the standing wave is formed by two detuned laser beams intersecting at an angle of  $70.4^\circ$ . The ultracold fermion atoms like the  $^{40}\text{K}$  is then loaded in the optical lattice [33]. The on-site interaction between the fermion atoms can be adjusted from zero to strong coupling limits by the Feshbach resonance. Using absorption imaging technology, the crucial physical quantities such as the double occupancy and the Fermi surface can be obtained to analyze the system [34].

In summary, we study the Mott transition of the interacting Dirac fermions on honeycomb lattice by CDMFT method. It is found that the low-energy density of states is independent of the interaction strength in the semimetal regime, hence the Fermi velocity always equals to the one of non-interacting Dirac sea. As the interaction increases, the system enters Mott insulator via a second-order phase transition accompanied by a pseudogap on the Fermi surface. This suggests the Mott transition is dominated by the Slater mechanism. It is also shown that the non-local correlations significantly reduce the low-energy density of states of the honeycomb lattice. We argue that because of lacking non-local correlations, the DMFT method is inadequate in the study of strongly correlated fermions on honeycomb lattice. Our study may contribute to the comprehension of the interaction driven Mott transition and the recently found quantum spin liquid on honeycomb lattice [5].

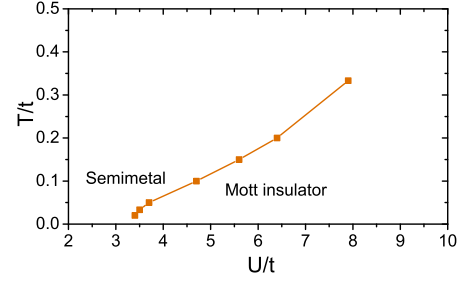


FIG. 6: (Color online) Phase diagram of the interacting Dirac fermions on honeycomb lattice. The line separating the semimetal and Mott insulator marks a second-order phase transition.

This work was supported by NSFC under grants Nos. 10874235, 10934010, 60978019, the NKBRSCF under grants Nos. 2006CB921400, 2007CB925004, 2009CB930701 and 2010CB922904. The numerical computations was done at the supercomputing center of CAS.

- 
- [1] K. S. Novoselov *et al.*, Science **306**, 666 (2004).
  - [2] C. L. Kane *et al.*, Phys. Rev. Lett. **95**, 226801 (2005).
  - [3] Y. Y. Zhang *et al.*, Phys. Rev. Lett. **102**, 106401 (2009).
  - [4] S. Raghu *et al.*, Phys. Rev. Lett. **100**, 156401 (2008).
  - [5] Z. Y. Meng *et al.*, Nature (London) **464**, 847 (2010).
  - [6] G. W. Semenoff, Phys. Rev. Lett. **53**, 2449 (1984).
  - [7] S. Sorella and E. Tosatti, Europhys. Lett. **19**, 699 (1992).
  - [8] C. Honerkamp, Phys. Rev. Lett. **100**, 146404 (2008).
  - [9] L. M. Martelo *et al.*, Z. Phys. B **103**, 335 (1997).
  - [10] W. Metzner *et al.*, Phys. Rev. Lett. **62**, 324 (1989).
  - [11] A. Georges and G. Kotliar, Phys. Rev. B **45**, 6479 (1992).
  - [12] R. Bulla, Phys. Rev. Lett. **83**, 136 (1999).
  - [13] A. Georges *et al.*, Rev. Mod. Phys. **68**, 13 (1996).
  - [14] G. Kotliar *et al.*, Phys. Rev. Lett. **87**, 186401 (2001).
  - [15] T. Maier *et al.*, Rev. Mod. Phys. **77**, 1027 (2005).
  - [16] N. H. Tong, Phys. Rev. B **72**, 115104 (2005).
  - [17] S. A. Jafari, Eur. Phys. J. B **68**, 537 (2009).
  - [18] M. T. Tran and K. Kuroki, Phys. Rev. B **79**, 125125 (2009).
  - [19] H. Park *et al.*, Phys. Rev. Lett. **101**, 186403 (2008).
  - [20] C. J. Bolech *et al.*, Phys. Rev. B **67**, 075110 (2003).
  - [21] A. N. Rubtsov *et al.*, Phys. Rev. B **72**, 035122 (2005).
  - [22] O. Parcollet *et al.*, Phys. Rev. Lett. **92**, 226402 (2004).
  - [23] T. Ohashi *et al.*, Phys. Rev. Lett. **100**, 076402 (2008).
  - [24] T. Ohashi *et al.*, Phys. Rev. Lett. **97**, 066401 (2006).
  - [25] J. E. Hirsch, Phys. Rev. B **31**, 4403 (1985).
  - [26] P. Werner *et al.*, Phys. Rev. Lett. **97**, 076405 (2006).
  - [27] S. W. Zhang *et al.*, Phys. Rev. Lett. **74**, 3652 (1995).
  - [28] M. Jarrell *et al.*, Phys. Rep. **269**, 133 (1996).
  - [29] G. Biroli and G. Kotliar, Phys. Rev. B **71**, 037102 (2005).
  - [30] M. Greiner *et al.*, Nature (London) **415**, 39 (2002).
  - [31] N. Gemelke *et al.*, Nature (London) **460**, 995 (2009).
  - [32] A. M. Dudarev *et al.*, Phys. Rev. Lett. **92**, 153005 (2004).
  - [33] L. M. Duan *et al.*, Phys. Rev. Lett. **91**, 090402 (2003).
  - [34] R. Jördans *et al.*, Nature (London) **455**, 204 (2008).